Available online at www.sciencedirect.com
SCIENCE DIRECT®
Physics of the Earth and Planetary Interiors 153 (2005) 3–10
PHYSICS OF THE EARTH AND PLANETARY INTERIORS
www.elsevier.com/locate/pepi

Low plume excess temperature and high core heat flux inferred from non-adiabatic geotherms in internally heated mantle circulation models

Hans-Peter Bunge*

Department of Earth Sciences, Ludwig Maximilians University Munich, D-80333 Munich, Germany

Received 23 November 2004; received in revised form 28 February 2005; accepted 21 March 2005

Abstract

Heat transfer across the core mantle boundary (CMB) is fundamentally important to Earth's internal energy budget. But the amount of heat entering the mantle from the core is poorly known. Classic arguments based on the dynamic topography over mantle hotspots suggest a rather modest core contribution to the mantle energy budget, on the order of 5–10%. Recent geodynamic studies, however, favor significantly higher values to overcome problems of insufficient internal mantle heat generation, and to satisfy constraints on the power requirements of the geodynamo and the thermal history of the core. Here, we use a high resolution mantle dynamics model to show that the non-adiabatic mantle geotherm which arises from internal mantle heating has an important effect in lowering the excess temperature of hot upwelling plumes by systematically decreasing the temperature differential between plumes and ambient mantle from the CMB toward the surface. This non-adiabatic effect of internally heated mantle flow may explain the unusually low plume excess temperatures inferred from the petrology of hotspot lavas, and implies current estimates of core heat flux based on hotspot topography should be raised perhaps by a factor of three.

Keywords: Heat flux; Core mantle boundary; Non-adiabatic geotherm

1. Introduction

1.1. Non-adiabaticity in the mantle geotherm

The average temperature increase through Earth's crust and mantle is called the geotherm. Its basic form is assumed to consist of adiabatic regions where temperatures rise only slightly with depth, and of narrow thermal boundary layers where temperatures increase rapidly over a depth of a few hundred kilometers (Jeanloz and Morris, 1986). In a noticeable paper, however, Jeanloz and Morris (1987) point out that the mantle geotherm away from thermal boundary layers should be shallower than the adiabat due to internal radioactive heat production: essentially as a volume element rises through the mantle its temperature decreases in response to adiabatic decompression. But at the same time its temperature increases due to internal heat released from radioactive decay, such that the net radial temperature change in internally heated mantle flow is smaller than the adiabatic gradient. Although there is considerable uncertainty, recently published analytic and computational mantle convection studies support the notion of non-adiabaticity in Earth's mantle, and most researchers have concluded that the mantle geotherm away from thermal boundary layers may depart by as much as 500 K from the adiabat (Bunge et al., 2001; Matyska and Yuen, 2000; Sleep, 2003).

We should have, of course, no expectation of an adiabatic thermal gradient in a fluid heated from within

* Tel.: +49 89 2180 4225; fax: +49 89 2180 4205.
E-mail address: bunge@lmu.de (H.P. Bunge)

0031-9201/$ – see front matter © 2005 Published by Elsevier B.V.
doi:10.1016/j.pepi.2005.03.017

(e.g., Richter and McKenzie, 1981) where the assumption of constant entropy is not valid. To estimate the non-adiabatic contribution to the mantle geotherm away from thermal boundary layers we follow a simple scaling argument (Sleep, 2003). Taking the heat equation, we have:

$$\rho C\left(\frac{\partial T}{\partial t}+\vec{u}\cdot\nabla T\right)=k\nabla^2 T+\rho H \tag{1}$$

where T, $\vec{u}$, t are temperature, velocity and time, respectively, ρ is the density, C and H are the specific heat and the internal heating rate per mass, and k is the thermal conductivity. Outside of thermal boundary layers, where thermal gradients are necessarily large, we may ignore the diffusive term as it is relatively small in Earth's mantle. Said differently, heat transport in the mantle is accomplished primarily by advection, so that Eq. (1) reduces to static heating by internal heat generation. Following a volume element through the mantle, we are left with:

$$\frac{\mathrm{D}T}{\mathrm{D}t}=\frac{H}{C} \tag{2}$$

where $\mathrm{D}T/\mathrm{D}t$ is the total time derivative moving with the volume element. For internally heated fluids all material must cycle through the upper thermal boundary layer (the lithosphere in mantle convection) to loose its heat. This situation differs from purely bottom heated fluids, where it suffices for material from the lower thermal boundary layer to cycle through the upper thermal boundary layer. We estimate the relevant time scale (Δt) in Eq. (2) from the geometry of plate tectonics. Taking the total length of the oceanic spreading system as 65,000 km and the average plate velocity as 5 cm/year, some 3 km^2 of ocean floor is created each year. If we assume that slabs and the material entrained with them are 200 km thick, admittedly this is an uncertain value, 600 km^3 material of mass 2×10^{15} kg enters the mantle (4×10^{24} kg) per year. At this rate the mantle cycles through the upper thermal boundary layer on a time scale $\Delta t_{\mathrm{mantle}}$ of order 2 billion years (Gyrs), which together with an assumed internal heating rate H of $10^{-11}\,\mathrm{W\,kg^{-1}}$ and a mantle heat capacity C of $1000\,\mathrm{J\,kg^{-1}\,K^{-1}}$ (Turcotte and Schubert, 2002) implies a non-adiabatic component (ΔT) of order 500 K in the mantle geotherm.

1.2. Heat transfer across the core mantle boundary

The notion of significant mantle non-adiabaticity has implications for the amount of heat transferred across the core mantle boundary (CMB), because it influences the effective temperature drop across the CMB (Bunge et al., 2001). There has been renewed attention lately to the ratio of internal mantle heat generation relative to the amount of heat that enters the mantle from the core. Geochemical arguments favor internal heating due to radioactive decay as the primary source in the mantle energy budget (Wasserburg et al., 1964). Classic arguments based on the dynamic topography over hotspots also suggest a modest core contribution to the mantle heat budget, on the order of 5–10% (Davies, 1988; Sleep, 1990). Recent geodynamic studies instead favor higher values to overcome problems of insufficient internal mantle heat sources (Kellogg et al., 1999), and to satisfy constraints on the power requirement of the geodynamo (Glatzmaier and Roberts, 1995; Kuang and Bloxham, 1997) and the thermal history of the core (Buffett, 2002; Nimmo et al., 2004). These studies receive further support from ab initio calculations, which permit alloying of iron and potassium in the core (Lee et al., 2004), although new results from numerical and laboratory dynamos have reappraised the power requirements of the geodynamo (Christensen and Tilgner, 2004).

1.3. The excess temperature of mantle plumes

Mantle non-adiabaticity might be detected directly from the temperature difference of mantle plumes relative to ambient mantle, the so-called excess temperature. It has been recognized for quite some time that the excess temperature in mantle plumes, inferred from petrologic studies to range around 200–300 K (Schilling, 1991), is low compared to independent estimates for a larger temperature change across the CMB (Jeanloz and Morris, 1986). If plumes originate from a thermal boundary layer at the CMB, this difference is difficult to understand. Farnetani (1997) showed that a chemically dense layer at the CMB helps to reduce the excess temperature of upwelling plumes by effectively buffering their temperature against the temperature of the core. The result suggests that chemical stratification across the CMB may govern the temperature of mantle plumes. We should, however, realize that relatively low plume excess temperatures are entirely expected for mantle convection with internal heat sources. We can understand why internal heating should lower the excess temperature of plumes if we look at the different time scales that govern the ascend of plumes relative to ambient mantle. While ambient mantle cycles through the upper thermal boundary layer over a time period $\Delta t_{\mathrm{mantle}}$ of order 2 Gyrs, as we saw before, plumes rise through the mantle on a shorter time scale $\Delta t_{\mathrm{plumes}}$ governed by the mantle transit time of order 100 million years. Consequently non-adiabatic effects due to internal heating are of minor importance

in upwelling plumes and plume temperatures follow the adiabat closely. The net result is that plumes start with a large excess temperature at the bottom of the mantle and that their excess temperature decreases systematically from the CMB toward Earth's surface.

In this paper, we explicitly study the effect of internal heating on the excess temperature of hot plume upwellings in mantle circulation models (MCMs) with mixed heating mode. We begin our study by introducing three simple MCMs having 5, 15 and 45% of their total surface heat flux, respectively, derived from core heating at the CMB. We present the bulk temperature distribution in these models compactly through the use of histograms. These histograms are 2-D contour plots of the total number of model grid points at any given temperature and at any given mantle depth. We find that the temperature differential (the excess temperature) between model grid points at average temperature (ambient mantle) and model grid points with a high temperature (plumes) decreases systematically from the bottom of the mantle upwards. The effect is particularly pronounced in models with high core heat flux. We go further by directly computing the excess temperature of hot upwellings relative to ambient mantle as a function of mantle depth. From this we find that the excess temperature drops by as much as a factor of three from the CMB toward the surface. We conclude our paper with the speculation that geodynamicists might have to raise their estimate of the core heat loss based on hotspot topography perhaps by a factor of three.

2. Mantle circulation models

2.1. Model setup

Fig. 1a shows the near surface and interior temperatures for a predominantly internally heated MCM (Bunge et al., 1998). The model is obtained by solving the usual mantle convection equations (Jarvis and McKenzie, 1980) for compressible flow at infinite Prandtl number (no inertial terms). Note that the viscosity increases by a factor of 40 from the upper to the lower mantle. The effect is known to have a strong influence on the convective planform (Bunge et al., 1996). But viscosity remains constant otherwise. We also include a factor 100 viscosity increase through the lithosphere (the upper 150 km in our model) relative to the upper mantle. Our modeling parameters, which are similar to a recently published study (Bunge et al., 2002), are listed in Table 1. We run the MCM for 4 Gyrs of Earth time (Bunge et al., 1997) until quasi-steady state is reached. We also assimilate a record of Mesozoic and Cenozoic plate motion (Lithgow-Bertelloni and Richards, 1998) sequentially as a surface velocity boundary condition where we scale the RMS velocity of the plate motion history to match the (slower) RMS surface velocity from the convection model. Put differently, the assimilated plate motion history neither increases nor impedes flow in our model calculation, and the model Peclet number remains unchanged. This sequential approach to data-assimilation in mantle convection models has been described in detail before (Bunge et al., 2002), and should be compared to more powerful data-assimilation methods based on a variational technique (Bunge et al., 2003).

Table 1
Model parameters

Parameter	Value
Outer shell radius (km)	6370
Inner shell radius (km)	3480
Numerical grid point resolution (surface) (km)	50
Numerical grid point resolution (CMB) (km)	25
T (surface) (K)	300
T (CMB) (for internally heated reference case) (K)	2800
Mantle density (surface) (kg m^{-3})	3500
Mantle density (CMB) (kg m^{-3})	5568
Coefficient of thermal expansion (surface) (K^{-1})	4.011×10^{-5}
Coefficient of thermal expansion (CMB) (K^{-1})	1.256×10^{-5}
Upper mantle dynamic viscosity $\eta_{\rm um}$ (Pa s)	1.0×10^{22}
Lower mantle dynamic viscosity	$40 \times \eta_{\rm um}$
Plate viscosity (upper 150 km of the mantle)	$100 \times \eta_{\rm um}$
Thermal conductivity (W m^{-1} K^{-1})	6.0
Internal heating rate (W kg^{-1})	6.0×10^{-12}
Heat capacity (J kg^{-1} K^{-1})	1134
Ra_H (based on $\eta_{\rm um}$)	10^8

To minimize the effect of unknown initial conditions we extend the data-assimilation back to pre-Mesozoic times by cyclically repeating the plate motion record through all Earth history. The vigor of mantle convection is governed by the non-dimensional Rayleigh number $Ra_{\rm int}$ (a buoyancy parameter) based on internal heating. $Ra_{\rm int}$ for Earth is probably of the order of 10^9 (Turcotte and Schubert, 2002). However, we choose $Ra_{\rm int} = 10^8$ in our model due to computational limitations, i.e. we cannot quite resolve the narrow thermal boundary layers in global mantle convection models at Earthlike Rayleigh numbers. We also include a modest 5% contribution of the total surface heat flux through bottom heating from the core. Since one cannot simultaneously specify both bottom heat flux and temperature, i.e. bottom heat flux is a model output for any given bottom temperature, we evaluated a large number of MCMs with core heat flux contributions ranging from zero (insulating) to 50%, and retained the model with 5% core heating. Geodynamicists regard this value as a lower bound for core heat flux,

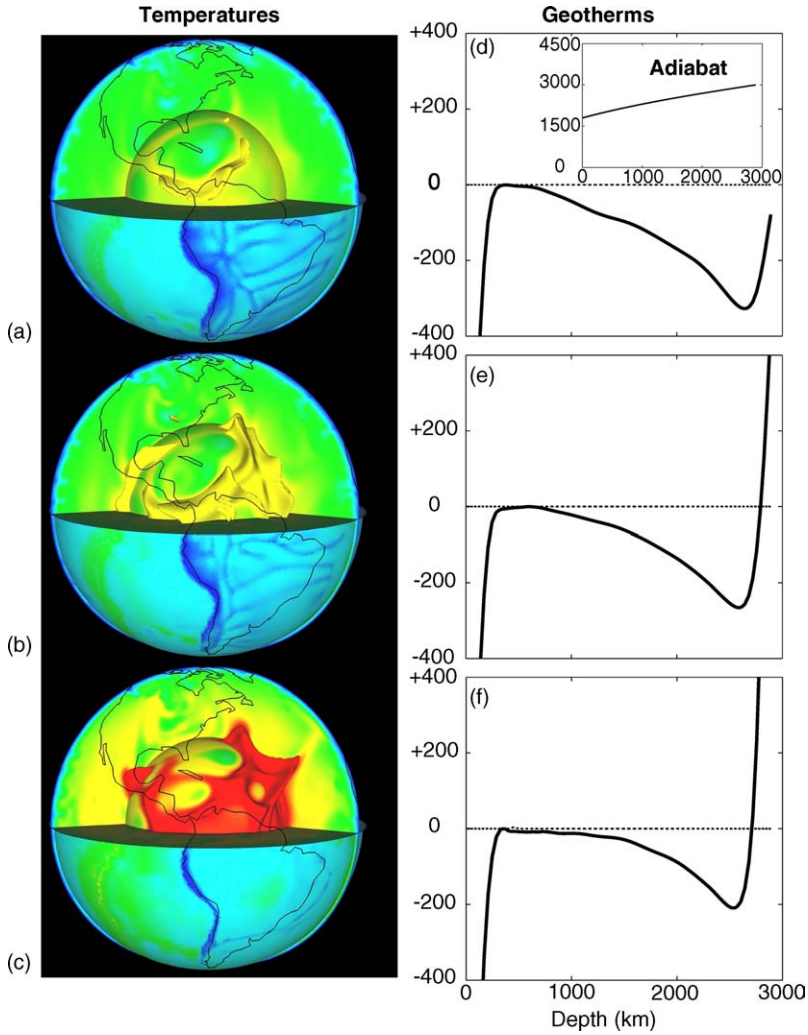

Fig. 1. (a) Temperature distribution for a predominantly internally heated reference mantle circulation model (see text) with $Ra_{\text{int}} = 10^8$. The view is centered on the American hemisphere and continental outlines are drawn for orientation. The linear color scale is identical for all models and ranges from 300 to 4000 K, where blue is cold and red is hot. The uppermost 100 km of the mantle is removed to show temperatures below the upper thermal boundary layer. An isosurface contours temperature values at 3500 K. Most of the mantle beneath the upper thermal boundary layer reveals uniform temperatures and a lack of hot upwelling plumes. (b) Same as (a), except for the addition of 15% core heat flux resulting in a moderate number of hot upwellings near the mantle base. (c) Same as (a), except for the addition of 45% core flux. The isosurface in this figure is pinned to 4000 K and there is a large number of hot upwelling plumes from the lower thermal boundary layer. (d–f) Non-adiabatic geotherms (see text) for cases (a–c). Superadiabaticity is concentrated into narrow thermal boundary layers near the top and bottom of the mantle. The geotherm is subadiabatic in intervening regions. Mantle subadiabaticity is strongest (about 400 K) in the predominantly internally heated reference model (a), and decreases in the models (b) and (c) with higher core heat flux. The inset figure (g) shows the model adiabat for comparison, plotted on a scale of 0–3000 km depth (x-axis) and 0–4500 K (y-axis). (For interpretation of the references to color in this figure legend, the reader is referred to the web version of this article.)

based on the global buoyancy flux inferred for mantle hotspots (Davies, 1988; Sleep, 1990).

2.2. *Non-adiabatic geotherms in internally heated mantle circulation models*

Fig. 1d shows the MCM geotherm. We subtract the reference adiabat (see figure inset) from the model geotherm to reveal the total non-adiabatic temperature change with depth. Note that in between the strongly superadiabatic upper and lower thermal boundary layers, mantle temperatures drop subadiabatically by about 400 K from the upper mantle to the CMB. Fig. 1b and c show two additional MCMs identical to the reference MCM in Fig. 1a, except that they include core heating rates of 15 and 45%, respectively, of the total surface

heat loss. These two models are representative for the range of more strongly bottom heated MCMs that we performed (see above), and show the effect of higher core heat flux. Model geotherms for these two MCMs are shown in Fig. 1e and f. In the intermediate MCM with 15% core heating (Fig. 1e) there is a total subadiabatic temperature drop from the upper mantle to the CMB of about 300 K, while the model with 45% core heating (Fig. 1f) reveals mantle subadiabaticity of about 200 K from the surface to the CMB, about half the value of the reference MCM in Fig. 1d.

It is logical to ask whether hot upwelling plumes reduce the mantle subadiabaticity in our MCMs with stronger core heat flux. We address this question in Fig. 2. Here, we plot histograms of MCM temperature versus depth, i.e. we contour the total number of model grid points at any given temperature (*x*-axis) as a function of mantle depth (*y*-axis). The reference MCM (Fig. 2a) reveals a narrow temperature distribution throughout the mantle. The contour plot shows a ridge where contour lines are tightly spaced both in the upper and the lower mantle. In other words, the temperature for the majority of model grid points clusters around values from about 1500 K in the upper mantle to about 2300 K in the lower mantle. There are also some model grid points where temperatures are lower by about 500 K relative to the bulk of the mantle. This is evidenced by a tail of contour lines to the left side of the ridge. The tail was noted in 2-D mantle convection models (Yanagisawa and Hamano, 1999) before. It is due to downwelling slabs (the cold upper thermal boundary layer of the mantle). The temperature reduction of about 500 K at these grid points is comparable to the temperature drop across the cold upper thermal boundary layer, as expected. Note that the histogram reveals nearly isothermal lower mantle temperatures, i.e. the bulk of the model grid points shows nearly constant temperature values (*x*-axis) as a function of mantle depth (*y*-axis). This agrees well with the reference MCM geotherm (Fig. 1d), where we saw strongly subadiabatic temperatures in the deepest mantle. The largest depth variation in the contour plot occurs near the surface. Here strongly superadiabatic temperatures characterize the upper thermal boundary layer, as expected for the predominantly internally heated flow in our model.

The temperature histogram for the MCM with 15% core heating (Fig. 2b) is similar to the reference MCM. However, in this model a significant depthwise change

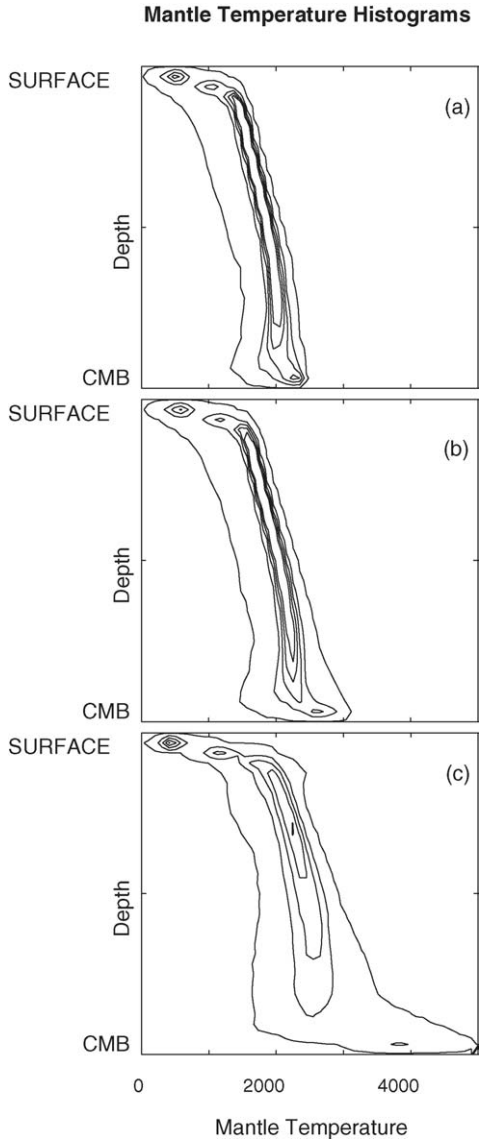

Fig. 2. (a) Contour plot of the bulk temperature distribution in the reference mantle circulation model, where the total number of model grid points at any given temperature (*x*-axis) is contoured as a function of mantle depth (*y*-axis). There are five contour lines spaced evenly at intervals of 17,440 model grid points, and starting from 3200 (the outer bold contour line) to 90,400 model grid points (the center contour line). The model temperature distribution is narrow and ridge like with a tight spacing of contour lines both in the upper and the lower mantle, and most model grid points cluster around temperature values ranging from about 1500 K in the upper to about about 2300 K in the lower mantle. There are also model grid points where temperatures are about 500 K lower than average, due to cold downwelling slabs (see text), as evidenced by contour lines to the left side of the ridge. Beneath the cold upper thermal boundary layer the contour plot reveals nearly isothermal mantle temperatures. (b/c) Same as (a) for the models with 15 and 45% core heating, respectively. Contour lines to the right side of the ridge reflect model grid points with warmer than average temperatures due to hot upwelling plumes. Note that the spacing of contour lines to the right side of the ridge narrows systematically away from the CMB. The effect is particularly pronounced in the model with high core heat flux (c) and reflects a systematic reduction in plume excess temperature relative to ambient mantle.

in the contour plot also occurs in the lowermost 200 km of the mantle. The contour plot shows a temperature rise by about 500 K in this region. Strongly superadiabatic temperatures at the bottom of the mantle characterize the lower thermal boundary layer, as expected for partly bottom heated flow. There are also model grid points in the lowermost mantle where temperatures are higher by about 500 K than average as evidenced by a tail of contour lines to the right side of the ridge. The tail is due to hot upwelling plumes. It is widest in the lowermost mantle and narrows progressively toward the surface.

We show the temperature histogram for the MCM with 45% core heating in Fig. 2c. The stronger bottom heating results in a stronger thermal boundary layer at the CMB, as expected. More importantly, there is now a wide tail of contour lines to the right side of the ridge with warmer than average model grid points due to upwelling plumes. The tail is broadest in the deepest mantle and narrows toward the surface, as we saw before in the model with 15% core heating. We understand this behavior in simple physical terms: plumes rise through the mantle relatively fast, especially in MCMs with strong core heating so that their radial temperature change is nearly adiabatic. The radial temperature variation in ambient mantle, instead, is nearly isothermal due to internal heating as we noted before. Thus the temperature difference (the excess temperature) between plumes and ambient mantle narrows systematically from the bottom toward the surface in our models.

2.3. Depth variation of plume excess temperatures

We quantify the plume-mantle temperature difference (the excess temperature) explicitly in Fig. 3. Here, we plot plume excess temperatures for the three MCMs as a function of mantle depth. To keep things simple we first compute a *hot geotherm* (G_h) by averaging at each radial level all model temperatures that lie 200 K and more above the mean mantle geotherm (G_m). We then subtract G_m from G_h. Recall that the excess temperature of mantle plumes at Earth's surface is probably no more than 200 K, based on the petrology of hotspot lavas (Schilling, 1991). So, our criterion for G_h reflects a physically plausible choice. Fig. 3a reveals that the excess temperature $G_h - G_m$ is nearly constant for our reference MCM with 5% core heating, reflecting the near absence of hot upwelling plumes. For the intermediate MCM with 15% core heating, Fig. 3b shows that $G_h - G_m$ decreases by about 100 K, with most of the change concentrated into the lowermost 1000 km of the mantle. This observation is in line with a visual inspection of the mantle temperature field (Fig. 1b), which reveals hot upwellings primarily near the mantle base. The most dramatic reduction in excess temperature occurs in the MCM with 45% core heat flux (Fig. 3c). In this case, $G_h - G_m$ decreases from

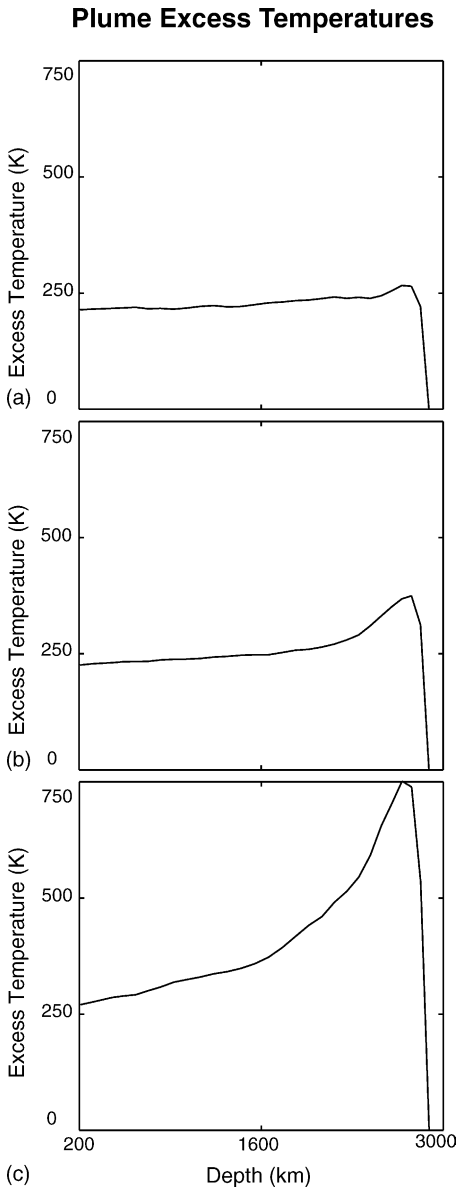

Fig. 3. (a) Plume excess temperature (see text) for the predominantly internally heated reference mantle circulation model (Fig 1a) shown as a function of mantle depth. The excess temperature is nearly constant, owing to the near absence of hot mantle upwellings in this model. (b) Same as (a) for the model with 15% core heating. Excess temperature decreases by 125 K, mostly in the lowermost 1000 km of the mantle. (c) Same as (a) for the model with 45% core heating. Plume excess temperature decreases systematically from 750 K near the CMB to 250 K near the surface. This is a three-fold reduction in plume excess temperature over the mantle depth.

about 750 K near the CMB to about 250 K near the surface. This represents a threefold drop in the plume excess temperature over the mantle depth.

3. Discussion and conclusion

Our calculations address a number of important related geodynamic problems. Geodynamicists have long noted that the petrologically inferred excess temperature of order 200–300 K for mantle plumes (Schilling, 1991) is much lower than geophysically plausible estimates for the temperature change across the CMB. The constraint that the outer core temperature must exceed the melting point of the iron alloy comprising the core suggests a much larger temperature rise across the thermal boundary layer at the CMB of order 1000 K (Jeanloz and Morris, 1986). The difference between these two estimates could be due in part to chemical stratification across D" (Farnetani, 1997). However, as far as we are aware our calculations show for the first time that low plume excess temperatures are entirely expected for internally heated mantle flow.

There is another consideration. Recent simulations of the geodynamo favor substantial heat flux across the CMB, on the order of 6–10 TW, to maintain convective criticality (Glatzmaier and Roberts, 1995; Kuang and Bloxham, 1997). Supporting independent evidence for a high core heat flux comes from thermal history studies of the core which require substantial internal core heat production to maintain plausible growth rates of the solid inner core (Buffett, 2002; Nimmo et al., 2004). Similarly, there is evidence from recent ab initio calculations on the alloying behavior of iron and potassium under high pressure conditions that permit the presence of potassium in the core (Lee et al., 2004). These arguments favor substantial heat transfer across the CMB. As a result some geodynamicists have argued for a higher core heat flux (Labrosse, 2002).

The main argument for a relatively low heat flux across the CMB, on the order of 2–3 TW, comes from buoyancy flux studies of mantle plumes constrained by the magnitude of hotspot swells (Davies, 1988; Sleep, 1990). While these studies have stood the test of time, our calculations show that both lines of argument could be reconciled. Our results suggest that estimates of the buoyancy flux carried by mantle plumes should account explicity for the effects of mantle non-adiabaticity. We verified for a large number of model calculations, where we varied the amount of core heat flux from zero to 50% of the total surface heat loss, that mantle non-adiabaticity of the order of 500 K is a robust feature of mantle convection with internal heating. Important independent confirmation of these results comes from recent analytic work which favors mantle subadiabaticity of comparable magnitude (Sleep, 2003). A systematic decrease of plume excess temperatures from about 750 K at the bottom of the mantle to about 250 K near Earth's surface, as suggested by our results, would go along with a threefold reduction of the apparent buoyancy flux carried by plumes through the mantle. The effect would help to bring the higher heat flux considerations of the geodynamo in line with the classic plume flux arguments based on dynamic topography over mantle hotspots.

The evidence from our calculations for a substantial depthwise increase in the excess temperature of plumes addresses, indirectly, two other problems in mantle dynamics. First, there are now numerous tomographic studies to show that slow seismic velocity anomalies indicative of mantle plumes are particularly prominent in the lowermost mantle (Dziewonski, 1984; Grand et al., 1997; van der Hilst et al., 1997; Ritsema et al., 1999; Boschi and Dziewonski, 1999). Recently, these lower mantle plumes have been linked directly to higher heat flux carried across the CMB (Romanowicz and Gung, 2002). The notion of strong plume flux in the mantle is supported further by novel tomographic modeling techniques which account for finite frequency effects (Montelli et al., 2004) and reveal a variety of lower mantle plumes. It is probably also related to independent evidence for ultra-low seismic velocities at the CMB (Garnero, 2000). Second, geochemical considerations suggest that the current mantle heat loss substantially exceeds the heat production rate from radioactive decay (Davies, 1999). The mantle heat imbalance could be closed if heat producing elements were concentrated into a dense basal layer in the lowermost mantle as suggested recently by Kellogg et al. (1999). But a higher core heat flux would offer a viable and simple alternative.

One shortcoming of our analysis is the somewhat arbitrary use of a 200 K cutoff to select for plume temperatures. The choice reflects the fact the excess temperature of mantle plumes is not well known. We could have used another cutoff to define the hot geotherm G_h. But our basic observation for a systematic decrease in the plume excess temperature (Fig. 3) would remain unchanged. The other main shortcoming of our models is the absence of horizontal viscosity variations due to thermal (or stress) variations (Tackley, 1993). Apart from further facilitating the rise of hot upwelling material due to a local reduction in the viscosity of plumes it is not obvious whether our main conclusions would be changed by modeling them. However, this question needs to be pursued in future studies.

Acknowledgment

We thank Geoff Davies for a constructive review.

References

Boschi, L., Dziewonski, A.M., 1999. High- and low-resolution images of the Earth's mantle: Implications of different approaches to tomographic modeling. J. Geophys. Res. 104 (25), 25–567, 594.

Bunge, H.-P., Richards, M.A., Baumgardner, J.R., 1996. Effect of depth-dependent viscosity on the planform of mantle convection. Nature 379, 436–438.

Bunge, H.-P., Richards, M.A., Baumgardner, J.R., 1997. A sensitivity study of three-dimensional spherical mantle convection at 10 (8) Rayleigh number. Effects of depth-dependent viscosity, heating mode, and an endothermic phase change. J. Geophys. Res. 102 11, 991–992 007.

Bunge, H.-P., Richards, M.A., Lithgow-Bertelloni, C., Baumgardner, J.R., Grand, S.P., Romanowicz, B., 1998. Time scales and heterogeneous structure in geodynamic earth models. Science 280, 91–95.

Bunge, H.-P., Ricard, Y., Matas, J., 2001. Non-adiabaticity in mantle convection. Geophys. Res. Lett. 28, 879–882.

Bunge, H.-P., Richards, M.A., Baumgardner, J.R., 2002. Mantle circulation models with sequential data assimilation: inferring present-day mantle structure from plate-motion histories. Philos. Trans. R. Soc., Ser. A 360, 2545–2567.

Bunge, H.P., Hagelberg, C.R., Travis, B.J., 2003. Mantle circulation models with variational data assimilation: inferring past mantle flow and structure from plate motion histories and seismic tomography. Geophys. J. Int. 152 (2), 280–301.

Buffett, B.A., 2002. Estimates of heat flow in the deep mantle based on the power requirements for the geodynamo. Geophys. Res. Lett., 29 (12): Art. No. doi:10.1029/2001GL014649.

Christensen, U.R., Tilgner, A., 2004. Power requirement of the geodynamo from ohmic losses in numerical and laboratory dynamos. Nature 429, 169–171.

Davies, G.F., 1988. Ocean bathymetry and mantle convection, 1. Large-scale flow and hotspots. J. Geophys. Res. 93, 10,467–10,480.

Davies, G.F., 1999. Dynamic Earth. Cambridge University Press, Cambridge, 470 p.

Dziewonski, A.M., 1984. Mapping the lower mantle. determination of lateral heterogeneity in P velocity up to degree and order 6. J. Geophys. Res. 89, 5929–5952.

Farnetani, C.G., 1997. Excess temperature of mantle plumes. The role of chemical stratification across D. Geophys. Res. Lett. 24, 1584–1586.

Garnero, E.J., 2000. Heterogeneity of the lowermost mantle. Annu. Rev. Earth Planet. Sci. 28, 509–537.

Glatzmaier, G.A., Roberts, P.H., 1995. A 3-dimensional self-consistent computer simulation of a geomagnetic field reversal. Nature 377, 203–209.

Grand, S.P., van der Hilst, R.D., Widiyantoro, S., 1997. Global seismic tomography: a snapshot of convection in the Earth. GSA Today 7, 1–7.

Jarvis, G.T., McKenzie, D.P., 1980. Convection in a compressible fluid with infinite Prandtl number. J. Fluid Mech. 96, 515–583.

Jeanloz, R., Morris, S., 1986. Temperature distribution in the crust and mantle. Annu. Rev. Earth Planet. Sci. 14, 377–415.

Jeanloz, R., Morris, S., 1987. Is the mantle geotherm subadiabatic. Geophys. Res. Lett. 14, 335–338.

Kellogg, L.H., Hager, B.H., van der Hilst, R.D., 1999. Compositional stratification in the deep mantle. Science 283, 1881–1884.

Kuang, W.L., Bloxham, J., 1997. An earth-like numerical dynamo model. Nature 389, 371–374.

Labrosse, S., 2002. Hotspots, mantle plumes and core heat loss. Earth Planet. Sci. Lett. 199, 147–156.

Lee, K.K.M., Steinle-Neumann, G., Jeanloz, R., 2004. Ab-initio high-pressure alloying of iron and potassium: Implications for the Earth's core. Geophys. Res. Lett. 31 (11): Art. No. L11603 2004.

Lithgow-Bertelloni, C., Richards, M.A., 1998. The dynamics of Cenozoic and Mesozoic plate motions. Rev. Geophys. 36, 27–78.

Matyska, C., Yuen, D.A., 2000. Profiles of the Bullen parameter from mantle convection modelling. Earth Planet. Sci. Lett. 178, 39–46.

Montelli, R., Nolet, G., Dahlen, F.A., Masters, G., Engdahl, E.R., Hung, S.-H., 2004. Finite frequency tomography reveals a variety of plumes in the mantle. Science 303, 338–343.

Nimmo, F., Price, G.D., Brodholt, J., Gubbins, D., 2004. The influence of potassium on core and geodynamo evolution. Geophys. J. Int. 156 (2), 363–376.

Richter, F.M., McKenzie, D.P., 1981. On some consequences and possible causes of layered mantle convection. J. Geophys. Res. 86, 6,133–6,142.

Ritsema, J., van Heijst, H.J., Woodhouse, J.H., 1999. Complex shear wave velocity structure imaged beneath Africa and Island. Science 286, 1,925–1,928.

Romanowicz, B., Gung, Y.C., 2002. Superplumes from the core-mantle boundary to the lithosphere: Implications for heat flux. Science 296, 513–516.

Schilling, J.-G., 1991. Fluxes and excess temperatures of mantle plumes inferred from their interaction with migrating mid-ocean ridges. Nature 352, 397–403.

Sleep, N.H., 1990. Hotspots and mantle plumes: Some phenomenology. J. Geophys. Res. 95, 6715–6736.

Sleep, N.H., 2003. Simple features of mantle-wide convection and the interpretation of lower-mantle tomograms. C. R. Geosci. 335, 9–22.

Tackley, P.J., 1993. Effects of strongly temperature-dependent viscosity on time-dependent, 3-dimensional models of mantle convection. Geophys. Res. Lett. 20, 2187–2190.

Turcotte, D.L., Schubert, G., 2002. Geodynamics. Cambridge University Press, Cambridge, 472 p.

van der Hilst, R.D., Widiyantoro, S., Engdahl, E.R., 1997. Evidence for deep mantle circulation from global tomography. Nature 386, 578–584.

Wasserburg, G.J., MacDonald, G.J.F., Hoyle, F., Fowler, W.A., 1964. Relative contributions of Uranium, Thorium, and Potassium to heat production in the Earth. Science 143, 465–467.

Yanagisawa, T., Hamano, Y., 1999. "Skewness" of S-wave velocity in the mantle. Geophys. Res. Lett. 26, 791–794.